Co-benefits of carbon neutrality in enhancing and stabilizing solar and wind energy

Yadong Lei[1], Zhili Wang[1], ... & Yangyang Xu[2] (presenter)

1 *Chinese Academy of Meteorological Sciences, Beijing, China* 2. Texas A&M University, College Station, TX

*Full list of a dozen authors at https://doi.org/10.1038/s41558-023-01692-7 or use the QR code to the right

Introduction

- Solar photovoltaic (PV) and wind energy provide carbon-free renewable energy to reach ambitious global carbon-neutrality goals, but their yields are in turn influenced by future climate change.
- Here, using a bias-corrected large ensemble of multi-model simulations under an envisioned post-pandemic green recovery, we find a general enhancement in solar PV over global land regions, especially in Asia, relative to the well-studied baseline scenario with modest climate change mitigation.
- Our results also show a notable west-to-east interhemispheric shift of wind energy by the mid-twenty-first century, under the two global carbon-neutral scenarios.
- Both solar PV and wind energy are projected to have a greater temporal stability in most land regions due to deep decarbonization.
- The co-benefits in enhancing and stabilizing renewable energy sources demonstrate a beneficial feedback in achieving global carbon neutrality and highlight Asian regions as a likely hotspot for renewable resources in future decades.

Methods

- CovidMIP simulation: Six ESMs participated in CovidMIP and we used four (ACCESS-ESM-5, MIROC-ES2L, MPI-ESM1-2-LR and MRI-ESM2-0). two carbon-neutral pathways from 2020 to 2050: a moderate green recovery (MOD) and a strong green recovery (STR)
- Bias correction: multivariate bias correction technique based on the n-dimensional probability density function transform (MBCn) to simultaneously correct daily T, I and W.

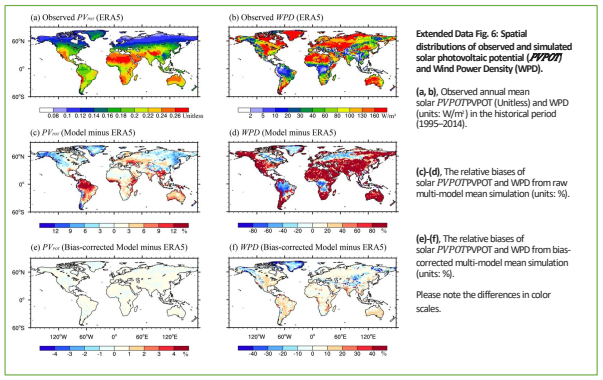

Extended Data Fig. 6: Spatial distributions of observed and simulated solar photovoltaic potential (*PVPOT*) and Wind Power Density (WPD).

(a, b), Observed annual mean solar *PVPOT*/PVPOT (Unitless) and WPD (units: W/m²) in the historical period (1995–2014).

(c)-(d), The relative biases of solar *PVPOT*/PVPOT and WPD from raw multi-model mean simulation (units: %).

(e)-(f), The relative biases of solar *PVPOT*/PVPOT and WPD from bias-corrected multi-model mean simulation (units: %).

Please note the differences in color scales.

generation. Following previous studies[13,43,62], we used daily T, I and W to calculate PV_{POT}:

$$PV_{POT} = P_R \frac{I}{I_{STC}} \quad (4)$$

where I represents surface downwelling shortwave radiation and I_{STC} represents shortwave flux on the PV panel under standard test conditions, defined as a constant of 1,000 W m^{-2}. P_R is the performance ratio, representing temperature influence on PV efficiency:

$$P_R = 1 + \gamma (T_{cell} - T_{STC}) \quad (5)$$

where γ is defined as −0.005 °C^{-1} in monocrystalline silicon solar panels, representing the negative impact on conversion efficiency, and T_{STC} is the cell temperature under standard test conditions (25 °C). T_{cell} is the actual cell temperature, which is approximated by T, I and W:

$$T_{cell} = \alpha 1 + \alpha 2 \times T + \alpha 3 \times I + \alpha 4 \times W \quad (6)$$

where $\alpha 1$, $\alpha 2$, $\alpha 3$ and $\alpha 4$ are taken as 4.3 °C, 0.943 (unitless), 0.028 °C (W m^{-2})$^{-1}$ and −1.528 °C (m s^{-1}), respectively. These coefficients represent the influence of meteorological

Calculation of wind energy

WPD (W m^{-2}) is a typical measure of wind energy potential[35], defined as follows:

$$WPD = \frac{1}{2}\rho W_h^3 \quad (7)$$

where ρ represents the air density, which is assumed to be a constant value of 1.213 kg m^{-3} at standard atmospheric conditions, and W_h represents the wind speed at the 100 m hub height.

It is noted that W_h is not available from climate model outputs here. Similar to previous studies[23,25], W_h is extrapolated from the 10 m wind speed (W) using the wind power law:

$$\frac{W_z}{W_{ref}} = \left(\frac{z}{z_{ref}}\right)^{\alpha} \quad (8)$$

where W_z represents the wind speed at a height z and W_{ref} represents the wind speed at a reference height z_{ref}. The scaling factor of α, representing how quickly the wind decays towards the ground, is often approximated as a constant of 0.143 over land surface in previous studies[23,26,45]. As the ERA5 reanalysis provided wind speeds at both 10 m and 100 m, here we estimate α at each location grid (Extended Data Fig. 7) to account for spatial disparity.

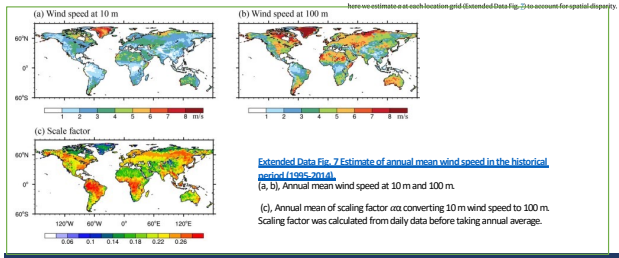

Extended Data Fig. 7 Estimate of annual mean wind speed in the historical period (1995-2014).
(a, b), Annual mean wind speed at 10 m and 100 m.

(c), Annual mean of scaling factor α converting 10 m wind speed to 100 m. Scaling factor was calculated from daily data before taking annual average.

Results

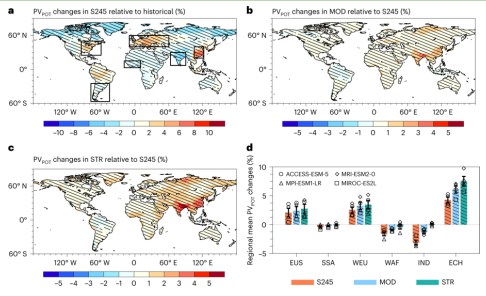

Fig. 1: Changes of solar PV_{POT}.
a, The relative changes of annual mean solar PVPOT (%) during 2040–2049 under SSP2-4.5 (S245) relative to the historical period.
b,c, The relative changes of annual mean solar PVPOT during 2040–2049 under the moderate (MOD; b) and strong (STR; c) mitigation scenarios relative to S245.
d, Regional mean relative changes of annual solar PVPOT during 2040–2049 under S245 (red bars), MOD (blue bars) and STR (green bars) scenarios, all relative to the historical period.

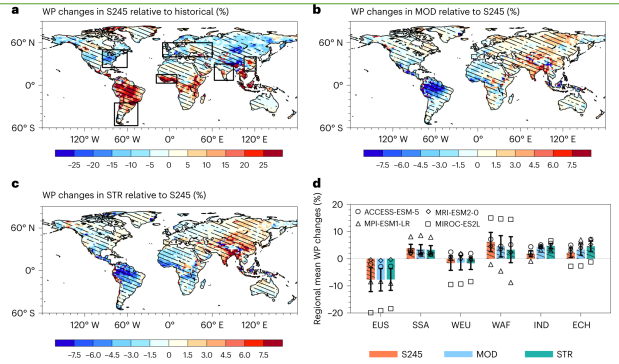

Fig. 3. Same as Fig. 1 but for wind energy.

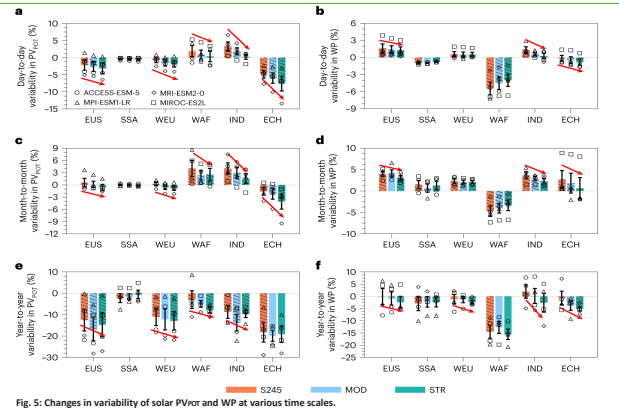

Fig. 5: Changes in variability of solar PV_{POT} and WP at various time scales.

a,**c**,**e**, The relative changes in day-to-day (**a**), month-to-month (**c**) and year-to-year (**e**) variability of solar PV_{POT} during 2040–2049 under S245 (red bars), MOD (blue bars) and STR (green bars) relative to the historical period.
b,**d**,**f**, The same but for relative changes in day-to-day (**b**), month-to-month (**d**) and year-to-year (**f**) variability of WP.

Results

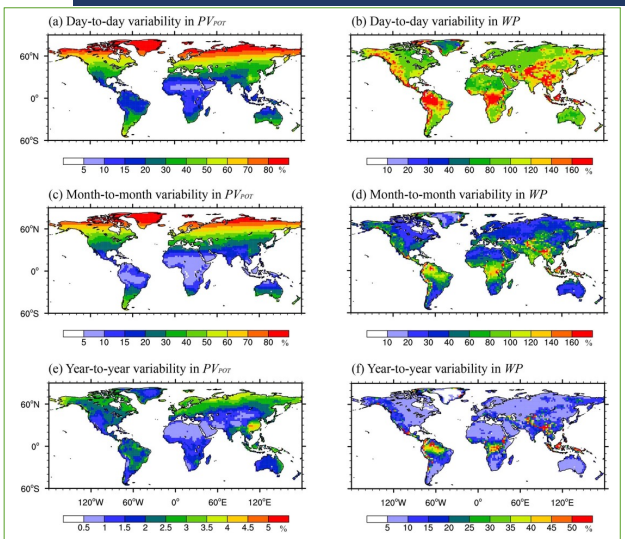

Extended Data Fig. 5: Variability of solar photovoltaic potential (*PVPOT*/PVPOT) and wind power (WP) at various time scales in the historical period.
(a), (c), and **(e)**, Day-to-day, month-to-month, and year-to-year variability of solar *PVPOT*/PVPOT in the historical period (units: %). **(b), (d),** and **(f)**, same as left panels but for WP.

Final thoughts

- Our results are valuable in making sound long-term plans of renewable investments across global regions.
- The findings that some regions are projected to observe large co-benefits of wind energy and solar PV associated with deep decarbonization could, in turn, support a faster clean energy transition to achieve the carbon-neutrality target, hence completing a favourable human–nature feedback loop.
- This is in stark contrast with previously reported detrimental feedback loops, for example, where global warming could reduce the potential capacity of bioenergy with carbon capture and storage[54], damaging the chances of meeting neutrality.
- In order to facilitate the transition into a global economy powered by clean energy, international coordination should be strengthened further, due to the spatial, temporal and technological imbalance of renewable energy resources.

References

- Forster, P. M. et al. Current and future global climate impacts resulting from COVID-19. *Nat. Clim. Change* **10**, 913–919 (2020).
- AlSkaif, T., Dev, S., Visser, L., Hossari, M. & van Sark, W. A systematic analysis of meteorological variables for PV output power estimation. *Renew. Energy* **153**, 12–22 (2020).
- Pryor, S. C., Barthelmie, R. J. & Schoof, J. T. Past and future wind climates over the contiguous USA based on the North American Regional Climate Change Assessment Program model suite. *J. Geophys. Res. Atmos.* **117**, D19119 (2012).
- Feron, S., Cordero, R. R., Damiani, A. & Jackson, R. B. Climate change extremes and photovoltaic power output. *Nat. Sustain.* **4**, 270–276 (2020).
- Gao, M. et al. Secular decrease of wind power potential in India associated with warming in the Indian Ocean. *Sci. Adv.* **4**, eaat5256 (2018).
- Karnauskas, K. B., Lundquist, J. K. & Zhang, L. Southward shift of the global wind energy resource under high carbon dioxide emissions. *Nat. Geosci.* **11**, 38–43 (2017).
- Pryor, S. C., Barthelmie, R. J., Bukovsky, M. S., Leung, L. R. & Sakaguchi, K. Climate change impacts on wind power generation. *Nat. Rev. Earth Environ.* **1**, 627–643 (2020).
- Gernaat, D. E. H. J. et al. Climate change impacts on renewable energy supply. *Nat. Clim. Change* **11**, 119–125 (2021).
- Hanna, R., Xu, Y. & Victor, D. G. After COVID-19, green investment must deliver jobs to get political traction. *Nature* **582**, 178–180 (2020).
- Hou, X., Wild, M., Folini, D., Kazadzis, S. & Wohland, J. Climate change impacts on solar power generation and its spatial variability in Europe based on CMIP6. *Earth Syst. Dyn.* **12**, 1099–1113 (2021).
- Chen, S. et al. Improved air quality in China can enhance solar-power performance and accelerate carbon-neutrality targets. *One Earth* **5**, 550–562 (2022).
- Lu, N. et al. High emission scenario substantially damages China's photovoltaic potential. *Geophys. Res. Lett.* **49**, e2022GL100068 (2022).
- Akinsanola, A. A., Ogunjobi, K. O., Abolude, A. T. & Salack, S. Projected changes in wind speed and wind energy potential over West Africa in CMIP6 models. *Environ. Res. Lett.* **16**, 044033 (2021).
- Cannon, A. J. Multivariate quantile mapping bias correction: an *N*-dimensional probability density function transform for climate model simulations of multiple variables. *Clim. Dyn.* **50**, 31–49 (2018).